Desalination and Water Treatment
www.deswater.com
doi: 10.5004/dwt.2023.29724

307 (2023) 1–7
September

Multi-action internal curve piston pump with energy recovery function for desalination system

Wenlei Li[a], Rui Guo[a,*], Guogang Wang[b], Jingyi Zhao[a], Qian Zhang[c], Lin Yu[b], Qisheng Zhang[a]

[a]*School of Mechanical Engineering, Yanshan University, Qinhuangdao 066004, China, emails: guorui@ysu.edu.cn (R. Guo), 1309116270@qq.com (W. Li), zjy@ysu.edu.cn (J. Zhao), 13933953612@ysu.edu.cn (Q. Zhang)*
[b]*Yongchunjie Seawater Desalination Technology Engineering Co., Ltd., Qinhuangdao 066004, China, emails: 13315668515@163.com (G. Wang), 13313333317@163.com (L. Yu)*
[c]*The Institute of Seawater Desalination and Multipurpose Utilization, MNR (Tianjin), 300192, China, email: sdzpzq@126.com*

Received 24 December 2022; Accepted 22 June 2023

ABSTRACT

The installed capacity of seawater reverse osmosis (SWRO) as the main means to solve the water resource crisis is increasing year by year. However, the current SWRO is mainly composed of membrane components, high pressure pumps, booster pumps and energy recovery devices. In this paper, a new multi-action internal curve seawater desalination high-pressure pump with energy recovery function was proposed, which can recover the pressure energy of concentrated seawater and pressurize the raw seawater at the same time. The working principle and internal structure of the pump were described in detail, and the design of a pulsation-free structure was illustrated. The operating pressure and specific energy consumption of the proposed system with different membrane component structures, feed water flow rate and recovery rate were analyzed. The final design of the membrane component structure had one segment for each stage with three containers in each segment and eight reverse osmosis membranes in each container. The recovery rate and the feedwater flow rate of the proposed system were 40% and 531 m^3/d, respectively. The specific energy consumption of water production reached 1.65 kWh/m^3 in a validation test. The water production cost and the system volume were both significantly reduced.

Keywords: Seawater desalination; Energy recovery; Specific energy consumption

1. Introduction

With the increase of population and the rapid development of industry, the demand for water resources is growing [1,2]. The shortage of water resources is becoming more and more serious. According to statistics, the world's per capita share of fresh water has halved in the past 50 y [3], 40% of the world's population is located within 100 km from the coastline, and desalination has become the most effective means to solve the water resource crisis [4,5]. From 2010 to 2019, the installed capacity of seawater desalination will grow steadily at a rate of 7%/y, 70% of which is seawater reverse osmosis (SWRO) system [6]. Reducing power consumption can greatly reduce the water production cost of reverse osmosis seawater desalination [7,8]. The extensive use of energy recovery devices and the improvement of membrane technology have reduced the specific energy consumption (SEC) of water production from 20 to 2 kWh/m^3 [9].

After decades of development, many scholars and commercial companies have proposed a variety of energy

* Corresponding author.

recovery devices (ERD). In view of the impact of reciprocating switcher energy recovery device (RS-ED) in the process of stroke switching, Jie et al. [10] proposed an improved RS-ED with pilot valve plate. The starting pressure was reduced by half, about 0.25 MPa, the pressure pulsation was reduced by 40%, and the device efficiency reached 98.5%. Yue et al. [11] propose a new single piston energy recovery device, which realizes the function of double cylinder energy recovery, and the energy recovery efficiency is 98%. Song et al. [12,13] proposed a hydraulic actuator, which has been proved to be reliable by simulation and experiment. The pressure fluctuation is 3%, and the energy recovery efficiency is 96%. He also proposed the emergency state control logic and strategy of the piston type energy recovery device. Abdollah carried out numerical analysis, design and simulation of the injector regulating valve and Pelton turbine impeller. The tests showed that the power was reduced by 26% compared with the absence of Pelton turbine [14]. ERD produced by Danfoss for small rainwater reverse osmosis device, which uses axial piston pump (APP) and axial piston motor (APM), with SEC ranging from 3 to 4.8 kWh/m^3 [15]. Dimitriou et al. [16] compared the SEC of SWRO system using different ERD, the minimum measured SEC of Clark SWRO device at 44 bar pressure is 5.7 kWh/m^3, while the minimum SEC of Danfoss SWRO device at 59 bar pressure is 4 kWh/m^3. Song et al. [17] has developed a new type of piston type integrated high-pressure pump energy recovery device (HPP-ERD) suitable for small SWRO system, developed three prototypes with water production flows of 2.166, 1.128 and 0.246 m^3/h, respectively, and the SEC of water production reaches 3.65, 4.37 and 5.25 kWh/m^3. William and Tzyy [18] proposed a centrifugal reverse osmosis (CRO) process, which uses the rotation of the module to generate centrifugal force. The centrifugal force increases the transmembrane pressure difference in varying degrees with the increase of the radial distance from the axis of symmetry, CRO can reduce the net specific energy consumption by 31% and the recovery rate is 50%, at 56 bar pressure of 35 g/L seawater feed. Zheng et al. [19] has developed a three cylinder energy recovery device (TC-ERD) and a matching control strategy with instantaneous overlapping function. The flow pulsation amplitude of low-pressure seawater (0.954 m^3/h) is 68.2% lower than that of RS-ERD, while the flow pulsation amplitude of high-pressure brine (1.336 m^3/h) is about twice that of RS-ERD. The energy recovery efficiency of TC-ERD is up to 97.1%.

In summary, the high-pressure pump, ERD and booster pump of the present SWRO system are separated, resulting in low system integration. Only Daiwang Song has developed a triple integrated high-pressure pump suitable for small SWRO, and the system has flow and pressure pulsations. In this paper, a new type of multi action internal curve seawater desalination high-pressure pump (MCPP-ER) with energy recovery function is proposed, that pressurize raw seawater without booster pump while recovering the pressure energy of concentrated seawater. Firstly, the working principle and structure of MCPP-ER are introduced in detail. Secondly, according to its output flow characteristics, the structure is designed without pulsation, and the system structure parameters are determined. Finally, the simulation test is carried out on the test bed.

2. Method

2.1. Description of working principle of the MCPP-ER

The MCPP-ER creatively integrates the energy recovery function inside the high-pressure pump, its working principle is shown in Fig. 1. The raw seawater and the concentrated seawater with pressure energy were simultaneously introduced into the pump. Fig. 2 displays the specific structure of the pump, which is composed of a stator, a rotor, a port plate, pistons, and related accessories.

In Fig. 1, the rodless end of the piston is the working chamber of the raw seawater, whereas the piston end with a rod is the working chamber of the concentrated seawater. Pistons 1, 4, 5, and 8 are operated to pressurize the raw seawater and recover the pressure energy of the concentrated seawater, whereas pistons 2, 3, 6, and 7 are used to induct the raw seawater and discharge the concentrated seawater.

The working process of the pump is illustrated using piston 1 as an example. The motor drives the rotor to rotate clockwise. The roller is always in contact with the

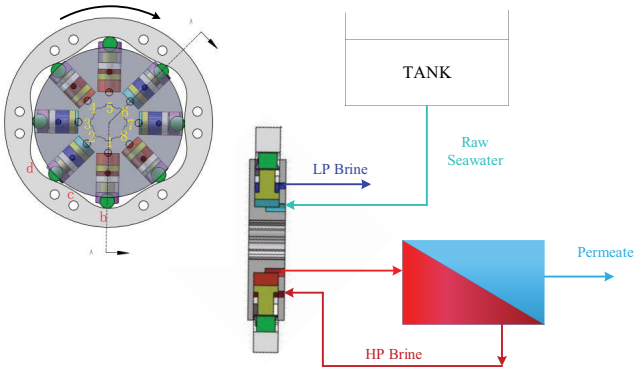

Fig. 1. Principle of MCPP-ER.

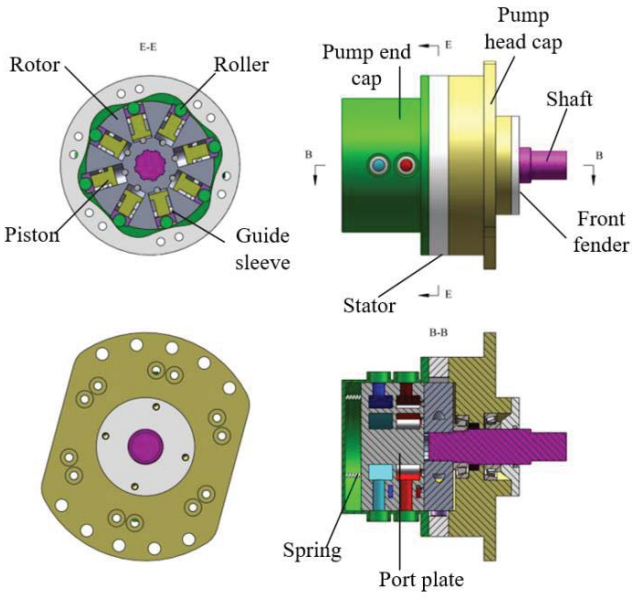

Fig. 2. Specific structure of MCPP-ER.

stator and moves along it. As the roller moves from the far point "b" to the near point "c", it forces piston 1 to retract in the radial direction along the rotor. The high-pressure concentrated seawater enters the rod end of the piston from the membrane through the port plate. The concentrated seawater exerts pressure on the annular area of the piston to provide a driving force for the piston to retract along the radial direction of the rotor. The mechanical energy provided by the motor gets combined with the pressure energy of the high-pressure concentrated seawater to pressurize the raw seawater. Subsequently, the feedwater pressure required by the membrane is achieved, and the pressurization of the raw seawater during the pressure energy recovery process of the concentrated seawater is realized. Piston 1 retracts completely as it approaches point "c". When piston 1 passes the near point "c", it starts to protrude outward, and the pre-treated raw seawater enters the rodless cavity through the port plate. The concentrated seawater is then discharged from the rod cavity into the port plate. As the rotor continues to rotate, piston 1 moves to the far point "d". At this moment, piston 1 is restored to the same phase as its initial position; thus, it completes the working cycle. The raw seawater flows into the rodless working chamber of piston 1 and flows out of the chamber through the port plate. Similarly, the concentrated sea water flows into the rod cavity and flows out of the chamber.

The proposed pump had six actions and eight pistons. During each revolution, each piston completed the following process cycle six times — raw seawater suction, raw seawater pressurization, pressure energy recovery of the high-pressure concentrated seawater, and concentrated seawater discharge. In order to meet the requirements of using eight pistons to handle the raw seawater and the concentrated seawater six times in one cycle, a new dual-layer flow plate with four fluid regions was designed, and its schematic diagram is displayed in Fig. 3, where the transparent part is a metal flow plate, the first layer contains the pressurized raw seawater area (red) and the high-pressure concentrated seawater area (yellow), and the second layer consists of the inducted raw seawater area (green) and the concentrated seawater area (blue). The rotor rotated relative to the stator and the port plate. The two working cavities of each piston on the rotor contacted the four fluid domains of the port plate alternately through the axial holes to complete the distribution of the raw seawater and the concentrated seawater.

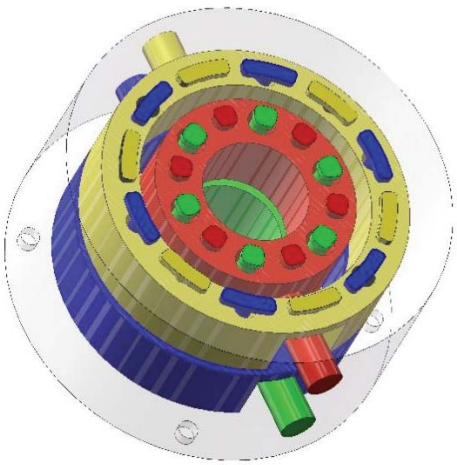

Fig. 3. Specific structure of port plate.

In SWRO system, the flow pulsation of high-pressure raw seawater directly affects the working life of reverse osmosis membrane components. Therefore, reducing or even eliminating the flow pulsation of raw seawater is of great significance to the whole system. Any instantaneous supply flow of raw seawater can be described by the following formula:

$$q_r = \sum_{i=1}^{z} \frac{\pi}{4} D^2 \times V_{\varphi i} \tag{1}$$

where q_r is the flow rate of raw seawater, z is the number of pistons, D is the piston diameter, $V_{\varphi i}$ is the speed of the piston relative to the rotor. To ensure uniform flow, the following equation must be satisfy:

$$\sum_{i=1}^{z} \frac{\pi}{4} D^2 \times V_{\varphi} = \text{cons} \tag{2}$$

Eq. (3) can be obtained by differentiating Eq. (2):

$$\frac{\pi}{4} D^2 \times \sum_{i=1}^{z} a_{\varphi} = 0 \tag{3}$$

where a_{φ} is the acceleration of the piston relative to the rotor.

Since the piston diameter is constant, as long as $\sum_{i=1}^{z} a_{\varphi} = 0$ is guaranteed, the feed flow of raw seawater can be absolutely uniform. The MCPP-ER proposed in this paper adopts the stator curve of the sinusoidal acceleration movement law. The suction and pressure out of raw seawater are arranged symmetrically. The first half cycle is the acceleration section and the second half cycle is the deceleration section. If the corresponding acceleration and deceleration section has the same phase piston entering or moving out at any moment, no pulsation can be guaranteed.

The MCPP-ER action angle proposed in this paper is $2\varphi_x = 2\pi/x = \pi/3$, As shown in Fig. 4, the amplitude angle of the acceleration zone is φ_1, the angle of deceleration area is φ_2, and the equation of stator curve can be described as follows:

$$a_{\varphi} = B\sin(\theta) \tag{4}$$

$$x\varphi_x = \pi \tag{5}$$

$$\frac{x}{\varphi_x} = \frac{\theta}{2\pi} \tag{6}$$

where x is the action times of stator curve.

Simultaneous Eqs. (4)–(6), so:

$$a_{\varphi} = B\sin(2x\varphi) \tag{7}$$

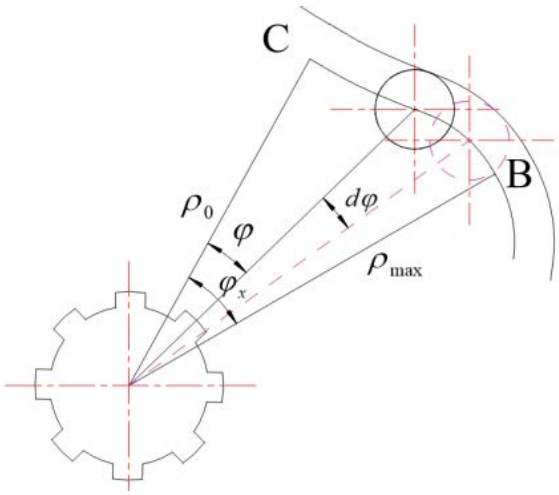

Fig. 4. Partial diagram of stator guide rail curve.

$$v_\varphi = \int B\sin(2x\varphi)d\varphi = -\frac{B}{2x}\cos(2x\varphi) + c_1 \tag{8}$$

$$\rho = \int V_\varphi d\varphi = \frac{B}{2x}\varphi - \frac{B}{4x^2}\sin(2x\varphi) + c_2 \tag{9}$$

Initial state, $\varphi = 0$, $V\varphi = 0$, $\rho = \rho_0$, according to Eq. (8), $c_1 = B/2x$ can be calculated, according to Eq. (9), $c_2 = \rho_0$ can be calculated.

$\Delta\rho$ can be described as follows:

$$\Delta\rho = \rho - \rho_0 = h = \frac{B}{2x}\times\frac{\pi}{6} - \frac{B}{4x^2}\times\sin\left(2x\times\frac{\pi}{6}\right) \tag{10}$$

where h is the stroke of the piston relative to the rotor.

The MCPP-ER output raw seawater flow of the pump can be described by the following formula:

$$Q_f = nV = n\frac{\pi}{4}D^2\times 6\times 8\times h \tag{11}$$

Different recovery rates can be adapted by changing the piston rod diameter, which can be described by the following formula:

$$\frac{A_r}{A_p} = \frac{D^2 - d^2}{D^2} = Y \tag{12}$$

where d is the diameter of the piston rod and Y is recovery rates.

2.2. Analysis working point of RO system

At present, the most widely used SWRO system is single-stage RO (SSRO). When the feed water pressure of raw seawater exceeds the thermodynamic osmotic pressure difference between the water on the salt side and the water on the desalination side of the rear end membrane (concentrated water outlet) of the reverse osmosis membrane module, the reverse osmosis process occurs. The osmotic pressure difference can be described by the following formula [20]:

$$\Delta p_\pi = \frac{\pi_0 R}{1 - Y} \tag{13}$$

where $\Delta p\pi$ is osmotic pressure difference, π_0 is the osmotic pressure generated by the salt content of the inlet water, R is the desalination rate of internal pressure reel type membrane.

The water flux of reverse osmosis membrane has a linear relationship with operating pressure and osmotic pressure difference, which can be expressed by the following equation [21,22]:

$$J_v = a\left(P_f - \Delta p_\pi\right) \tag{14}$$

where J_v is water flux, a is the desalination rate of membrane, P_f is the pressure of raw seawater.

The water production capacity of reverse osmosis membrane system can be described by the following formula:

$$Q_p = J_v A \tag{15}$$

where Q_p is the flow rate of product water, and A is the reverse osmosis membrane area.

In SWRO, the main cost is power consumption, and its energy consumption can be expressed in terms of system SEC, which is defined as how much electricity is consumed per cubic meter of fresh water, and can be described by the following equation:

$$\text{SEC} = \frac{P_f Q_f \times 1{,}000}{60 Q_P \times 60 \times \eta} \tag{16}$$

where η is total efficiency.

The MCPP-ER proposed in this paper replaces the high-pressure pump, ERD and booster pump. The specific energy consumption of the integrated system can be described by the following formula:

$$\text{SEC}_{\text{net}} = \frac{\left(P_f Q_f - P_b\left(1 - Y\right)Q_f\right)\times 1{,}000}{Q_f Y \times 60 \times 60 \times \eta} \tag{17}$$

The SEC of water production was closely related to the system structure, such as the number of membranes, stages, and segments and also the recovery rate. The optimal working point, which had the lowest specific energy consumption, was found through different system structural configurations and the proper selection of the recovery rate. In order to achieve a raw seawater flow rate of 366 L/min from the proposed piston pump, a Dow desalination membrane SW30XHR-400i was selected to compose membrane components with different structures. The system performance was analyzed with different parameters.

Fig. 5 depicts the feedwater pressure distribution affected by the number of reverse osmosis membranes and the

recovery rate. It is observable that when the recovery rate was constant and the number of reverse osmosis membranes increased, the feedwater pressure gradually decreased. It happened because the flow area of the system increased at the raw seawater flow rate of 366 L/min. Similarly, when the number of reverse osmosis membranes was constant, the feedwater pressure increased with the rise of the recovery rate because the increased recovery rate caused an increment in the osmotic pressure difference. When the number of reverse osmosis membranes was small and the recovery rate was high, the feedwater pressure exceeded 80 bar, which surpassed the maximum pressure that the reverse osmosis membrane could sustain. Hence, this system structure is not viable under such a scenario.

Fig. 6 presents the pressure difference distribution of the concentrated water. Two peaks occurred when the number of membranes was 10 and the recovery rate was 45%. When the number of membranes was 16 and the recovery rate was 40%, the pressure difference reached 3 bar. When the number of membranes was 25 and the recovery rate was 55%, the pressure difference reached the lowest value of 0.25 bar.

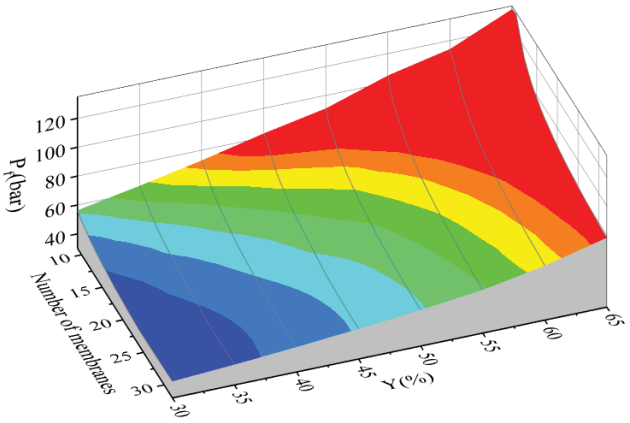

Fig. 5. Distribution of feed water pressure.

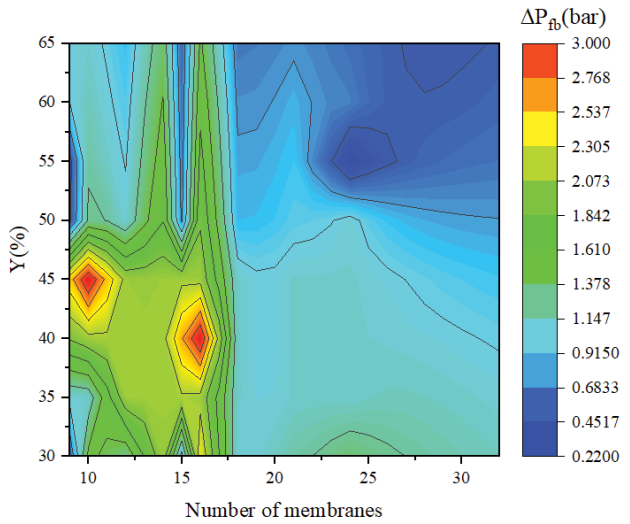

Fig. 6. Isosurface of concentrated water pressure difference.

Fig. 7 exhibits the distribution of the SEC of water production calculated with 80% efficiency. The lowest value was detected when the number of reverse osmosis membranes was 32 and the recovery rate was 55%. It is evident from Figs. 4–6 that when the number of reverse osmosis membranes was 24, a low water production pressure, a small pressure difference between the feedwater and the concentrated water, and a low specific energy consumption of water production were achieved. With the consideration that the energy recovery power was inversely proportional to the pressure difference and the recovery rate, the membrane component structure was determined to have one segment in each stage with three containers in each segment and eight reverse osmosis membranes in each container.

3. Results and discussion

According to the proposed membrane assembly structure, several pistons with different area ratios were machined to accommodate different recovery rates. The energy recovery effect and specific energy consumption of the seawater desalination pump with different recovery rates were experimentally analyzed. The principle of the experiment is illustrated in Fig. 8, and the experimental device is displayed in Fig. 9. A closed-loop control was formed by the pressure sensor and the flow rate sensor at the outlet of the variable displacement pump to ensure that the flow rate and pressure characteristics of the concentrated seawater were properly simulated. The speed sensor and the torque sensor between the motor and the MCPP-ER were used to monitor the input power of the MCPP-ER. The output power of the MCPP-ER was calculated using the data of pressure sensor 1 and flow rate sensor 2.

Fig. 10 exhibits the pressure and flow rate curves of the raw seawater. As the starter motor slowly accelerated, the flow rate gradually increased and became stabilized at 344 L/

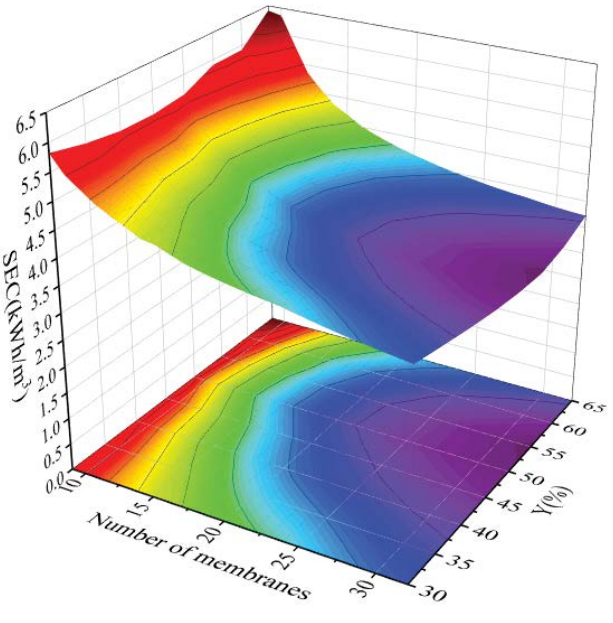

Fig. 7. Distribution of SEC.

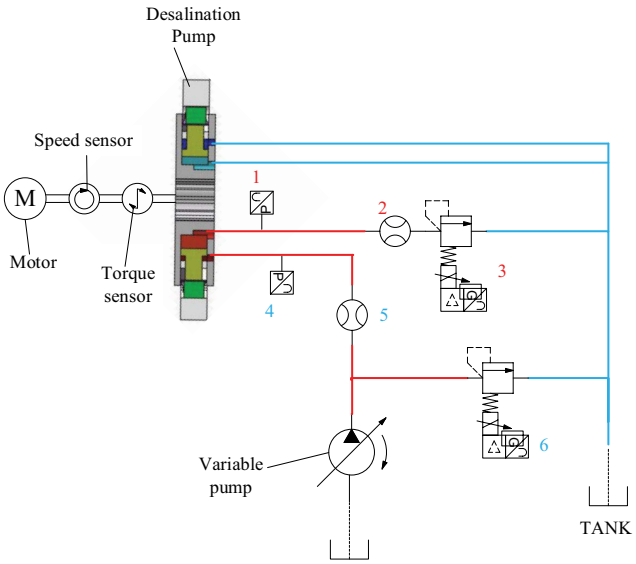

Fig. 8. Schematic diagram, 1. Pressure sensor; 2. Flow sensor; 3. Proportional relief valve; 4. Pressure sensor; 5. Flow sensor; 6. Proportional relief valve.

Fig. 9. Test experimental device.

min with almost no flow pulsations in the steady state. The pressure rapidly increased to 5 MPa with an overshot and a peak of 5.4 MPa, and it happened because the instant output flow of the pump reached the relief valve and caused impacts and vibrations. As the pressure of relief valve 3 was set at 5 MPa, when the pressure of the raw seawater reached 5 MPa, the raw seawater overflowed back into the tank. At this moment, the raw seawater outputted by the pump returned to the tank from the relief valve.

In the first stage, the working condition of recovering pressure energy from concentrated seawater is simulated, and the pressure of concentrated seawater is set to 0 MPa, which is realized through proportional relief valve 6. In the second stage, the simulation seawater desalination pump starts to recover the pressure energy in the concentrated seawater, and the pressure of the concentrated seawater output by the variable displacement pump is set to 4.8 MPa

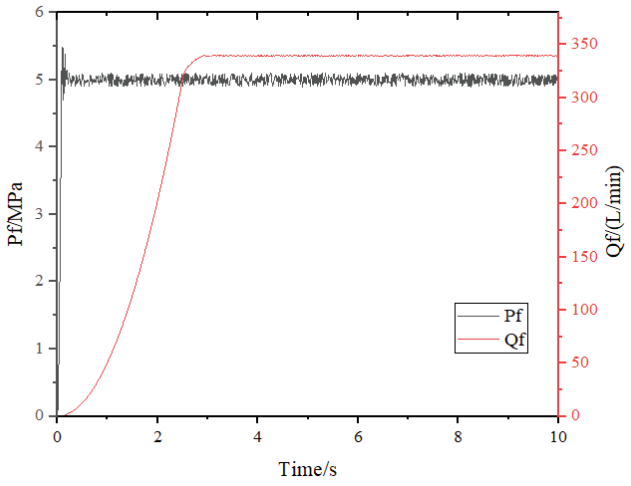

Fig. 10. Pressure and flow curve of feed water.

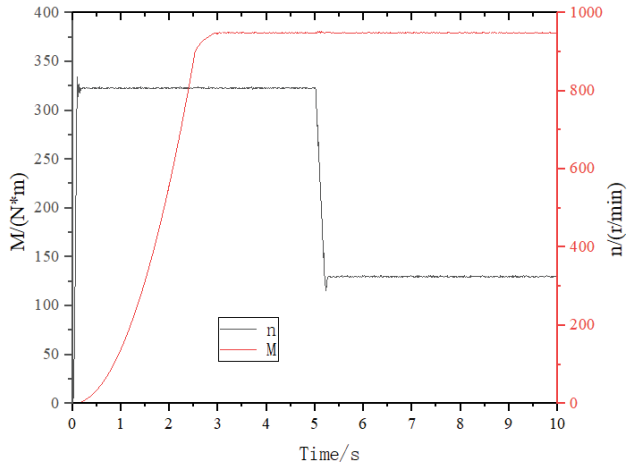

Fig. 11. Motor output speed and torque curve.

through the proportional relief valve 6. It can be seen from Fig. 9 that in 5 s, the motor output torque drops step by step from 323 to 130 N·m, producing a downward peak, The reason is that the set pressure of proportional relief valve 6 suddenly jumps from 0 to 4.8 MPa under the action of electrical signal, which causes overshoot under the action of fluid inertia. The corresponding concentrated seawater pressure can rise to the peak value instantly, and the motor torque decreases; At the same time, the motor speed rises instantaneously and is rapidly stabilized at 950 rpm under control.

Fig. 11 shows the output torque and speed of the motor measured by the speed-torque sensor, that is, the input speed and torque of the MCPP-ER pump. In the first stage, the pressure of the concentrated seawater was set at 0 MPa by adjusting the proportional relief valve 6, the pressure energy in the concentrated seawater that was not recovered was simulated. In the second stage, the energy recovery of the concentrated seawater in the pump was simulated. The concentrated seawater pressure output by the variable pump was set at 4.8 MPa by adjusting the proportional

relief valve 6. It is noticeable from Fig. 11 that the motor output torque decreased stepwise from 323 to 130 N·m in five seconds, producing a downward valley. It happened because the set pressure of proportional relief valve 6 suddenly jumped from 0 to 4.8 MPa under the action of electrical signals; thus, an overshoot was produced with the fluid inertia. Therefore, the corresponding pressure of the concentrated seawater reached rapidly the peak value, and the motor torque decreased. Subsequently, the motor speed increased quickly and became stabilized at 950 r/min under electronic control.

The pressure of proportional relief valve 6 was adjusted to simulate the turning-off and turning-on of the energy recovery function of the desalination pump. The energy saving of the proposed desalination pump was calculated as:

$$\eta_r = n\frac{M_f - M_c}{M_f} \times 100\% \tag{18}$$

where η_r is energy saving rate, n is the speed of motor, M_f is normal torque, M_c is the motor torque after energy recovery.

The simulated test data revealed that the energy saving of the MCPP-ER with the pressure energy recovery function was 58.6%. The total efficiency of the proposed pump was obtained using the ratio of the total output power to the total input power, and the value reached 89.2%. The specific energy consumption of water production of the proposed MCPP-ER reached 1.65 kWh/m^3 with a 40% recovery rate [calculated by Eq. (17)].

4. Conclusion

In order to meet the demand for pressure energy recovery of the concentrated seawater in reverse osmosis desalination systems, a new principle and structure of the MCPP-ER is proposed. The pump had the functionalities of pressurization and energy recovery. The pulsating output was realized through the internal structure analysis of the system. A simulated test bench was designed to validate the feasibility of the proposed pump. The specific energy consumption of water production was achieved as low as 1.65 kWh/m^3 with the proposed membrane component structure, which had one segment in each stage with three containers in each segment and eight reverse osmosis membranes in each container.

Acknowledgement

This research was supported by Qinhuangdao Yongchunjie Seawater Desalination Technology Engineering Co., Ltd and The Institute of Seawater Desalination and Multipurpose Utilization.

References

[1] W.L. Ang, A.W. Mohammad, N. Hilal, C.P. Leo, A review on the applicability of integrated/hybrid membrane processes in water treatment and desalination plants, Desalination, 363 (2015) 2–8.
[2] T. Distefano, S. Kelly, Are we in deep water? water scarcity and its limits to economic growth, Ecol. Econ., 146 (2018) 130–147.
[3] A. Zapata-Sierra, M. Cascajares, A. Alfredo, F. Manzano-Agugliaro, Worldwide research trends on desalination, Desalination, 519 (2022) 115305, doi: 10.1016/j.desal.2021.115305.
[4] P.S. Goh, T. Matsuura, A.F. Ismail, N. Hilal, Recent trends in membranes and membrane processes for desalination, Desalination, 391 (2016) 43–60.
[5] H. Shemer, R. Semiat, Sustainable RO desalination – energy demand and environmental impact, Desalination, 424 (2017) 10–16.
[6] J. Eke, A. Yusuf, A. Giwa, A. Sodiq, The global status of desalination: an assessment of current desalination technologies, plants and capacity, Desalination, 495 (2020) 114633, doi: 10.1016/j.desal.2020.114633.
[7] M. Göktuğ Ahunbay, Achieving high water recovery at low pressure in reverse osmosis processes for seawater desalination, Desalination, 465 (2019) 58–68.
[8] H. Sakai, T. Ueyama, M. Irie, K. Matsuyama, A. Tanioka, K. Saito, A. Kumano, Energy recovery by PRO in sea water desalination plant, Desalination, 389 (2016) 52–57.
[9] A.M. Blanco-Marigorta, A. Lozano-Medina, J.D. Marcos, A critical review of definitions for exergetic efficiency in reverse osmosis desalination plants, Energy, 137 (2017) 752–760.
[10] Z. Jie, W. Yue, F. Zhong, Z.S. He, S.C. Xu, Effective modifications of reciprocating-switcher energy recovery device by adopting pilot port plates to decrease the switching load and fluid fluctuations, Desalination, 462 (2019) 39–47.
[11] W. Yue, R. Yafei, Z. Jie, E. Xu, S. Xu, Functionality test of an innovative single-cylinder energy recovery device for SWRO desalination system, Desalination, 388 (2016) 22–28.
[12] D.W. Song, Y. Wang, S.C. Xu, J.P. Gao, Y.F. Ren, S.C. Wang, Analysis, experiment and application of a power-saving actuator applied in the piston type energy recovery device, Desalination, 361 (2015) 65–71.
[13] D.W. Song, Y. Wang, S.C. Xu, Z.C. Wang, H. Liu, S.C. Wang, Control logic and strategy for emergency condition of piston type energy recovery device, Desalination, 348 (2014) 1–7.
[14] A.E. Sani, Design and synchronizing of Pelton turbine with centrifugal pump in RO package, Energy, 172 (2019) 787–793.
[15] L.S. Drabløs, Testing of DanfossAPP1.0–2.2 with APP pumps as water hydraulic motors for energy recovery, Desalination, 183 (2005) 41–54.
[16] E. Dimitriou, E.S. Mohamed, C. Karavas, G. Papadakis, Experimental comparison of the performance of two reverse osmosis desalination units equipped with different energy recovery devices, Desal. Water Treat., 55 (2015) 3019–3026.
[17] D.W. Song, Y. Zhang, H.T. Wang, L.D. Jiang, C.P. Wang, S.H. Wang, Z.G. Jiang, H. Li, Demonstration of a piston type integrated high pressure pump-energy recovery device for reverse osmosis desalination system, Desalination, 507 (2021) 115033, doi: 10.1016/j.desal.2021.115033.
[18] B.K. William, H.C. Tzyy, Centrifugal reverse osmosis (CRO) − a novel energy-efficient membrane process for desalination near local thermodynamic equilibrium, J. Membr. Sci., 637 (2021) 119630, doi: 10.1016/j.memsci.2021.119630.
[19] S. Zheng, Y. Wang, J. Zhou, Z.T. Xu, S.C. Xu, Development and operational stability evaluation of new three-cylinder energy recovery device for SWRO desalination system, Desalination, 502 (2021) 114909, doi: 10.1016/j.desal.2020.114909.
[20] A.H. Zhu, P.D. Christofides, Y. Cohen, Minimization of energy consumption for a two-pass membrane desalination: effect of energy recovery, membrane rejection and retentate recycling, J. Membr. Sci., 339 (2009) 126–137.
[21] T.Y. Qiu, A.P. Davies, Concentration polarization model of spiral-wound membrane modules with application to batch-model RO desalination of brackish water, Desalination, 368 (2015) 36–47.
[22] S. Senthil, S. Senthilmurugan, Reverse osmosis–pressure retarded osmosis hybrid system: modelling, simulation and optimization, Desalination, 389 (2016) 78–97.